GEOLOGY | THE GEOLOGICAL SOCIETY OF AMERICA®

https://doi.org/10.1130/G51793.1

Manuscript received 11 October 2023
Revised manuscript received 12 January 2024
Manuscript accepted 29 January 2024

Published online 15 February 2024

Discovery of modern living intertidal stromatolites on Sheybarah Island, Red Sea, Saudi Arabia

Volker Vahrenkamp[1,*,†], Viswasanthi Chandra[1,†], Elisa Garuglieri[2], Ramona Marasco[2], Kai Hachmann[1], Pankaj Khanna[3], Daniele Daffonchio[2], and Alexander Petrovic[1,4]

[1]Physical Sciences and Engineering Division (PSE), King Abdullah University of Science and Technology, 4700 KAUST, Thuwal 23955-6900, Saudi Arabia

[2]Biological and Environmental Sciences and Engineering Division (BESE), King Abdullah University of Science and Technology, 4700 KAUST, Thuwal 23955-6900, Saudi Arabia

[3]Department of Earth Sciences, Indian Institute of Technology Gandhinagar, Palaj, Gandhinagar 382055, Gujarat, India

[4]Carmeuse SA, 5300 Seilles, Belgium

ABSTRACT

Microbial carbonates, and stromatolites in particular, represent the earliest geological record of life on Earth, which dominated the planet as the sole biotic carbonate factory for almost 3 b.y., from the Archean to the late Proterozoic. Rare and sparsely scattered across the globe in the present day, modern "living" stromatolites are typically relegated to extreme environmental niches, remaining as vestiges of a prodigious microbial past. Here, we report the first discovery of living shallow-marine stromatolites in the Middle East, on Sheybarah Island, Al Wajh carbonate platform, on the NE Red Sea shelf (Saudi Arabia). We detail their regional distribution and describe their environmental conditions, internal structures, and microbial diversity. We also report the first discovery of reticulated filaments in a photic setting, associated with these stromatolites. The Sheybarah stromatolites occur in the intertidal to shallow subtidal zones along the seaward-facing beach in three depth-dependent growth forms. Their inner layers were formed by microbially mediated accretion and differential lithification of sediment grains. Compositional microbial analysis revealed the presence of a wide range of microbial life forms.

INTRODUCTION

Stromatolites are a vestige of the first life on Earth, dominating carbonate-forming marine biota in the Archean and Proterozoic (Grotzinger and Knoll, 1999). Recent evidence dates the earliest occurrence of stromatolites to 3.48 Ga (Hickman-Lewis et al., 2023). With the exception of a few short intervals during the Phanerozoic, their importance in producing carbonates in modern times has been reduced to niche occurrences found predominantly in challenging environments, such as hypersaline marine settings and alkaline lakes (Carvalho et al., 2018; Samylina and Zaytseva, 2019; Marin-Carbonne et al., 2022). Understanding how lithified stromatolites form, which microbes contribute to growth processes, and how nutrient cycling works would provide insights into early life and ocean evolution on Earth, and perhaps on other planets, such as Mars. So far, the only occurrences of modern open-marine stromatolites are in the Exuma islands of the Bahamas (Dill et al., 1986; Visscher et al., 1998; Reid et al., 1995, 2000) and in Shark Bay, Australia (Suosaari et al., 2016, 2019). Here, we report the discovery of living stromatolites on Sheybarah Island, Red Sea, Saudi Arabia (Fig. 1). Although the presence of ancient microbialites (Perri et al., 2018; Strohmenger and Jameson, 2018) and microbial mats (Bontognali et al., 2010) has been previously recorded in the Middle East, this is the first record of modern intertidal stromatolites in this region.

GEOLOGICAL SETTING

The newly discovered stromatolites are located on SW Sheybarah Island of the Al Wajh carbonate platform along the NW coast of Saudi Arabia (Figs. 1A and 1B). The land-attached Al Wajh platform is located in the NE Red Sea and is almost completely enclosed by a 115 km reef-shoal belt (Petrovic et al., 2022). The platform hosts a 42-m-deep lagoon that is characterized by 92 islands and patch reefs of varying size. Sheybarah Island, with an area of 27 km^2 and a maximum elevation of 2 m above mean sea level, is situated on the SW edge of the platform (Fig. 1B). The southern slope of the platform is characterized by extensive mangrove forest mainly on the lagoon-facing rim, a sandy and rocky interior, carbonate beach sand ridges, skeletal carbonate sand, and rocky reef flats facing the open sea (Chalastani et al., 2020; Petrovic et al., 2023a). The semi-enclosed and oligotrophic Red Sea is characterized by poor water exchange and slow surface-water renewal (Maillard and Soliman, 1986). In the NE Red Sea, the average sea-surface temperature ranges between 28 °C in summer and 23 ± 1 °C during winter, while sea-surface salinities can reach up to 41‰. The prevailing wind direction is NNW with an average speed of 4 m s^{-1} (1980–2015; Dasari et al., 2018; Petrovic et al., 2023b), while during wintertime, strong SW winds occasionally occur (Fig. 1C; Raitsos et al., 2013). In addition, strong eastward-blowing zonal winds transport Fe-rich eolian sediments to the Red Sea realm, alternating with westward-blowing zonal winds during summer (Jiang et al., 2009).

METHODS

The first fieldwork that led to the discovery of the stromatolite field was conducted using a small local fishing boat during a scouting visit to Sheybarah Island in January 2021. Detailed descriptions of field visits and sampling and data

Volker Vahrenkamp https://orcid.org/0000-0002-2182-7993

*volker.vahrenkamp@kaust.edu.sa

†V. Vahrenkamp and V. Chandra contributed equally as co-first authors.

CITATION: Vahrenkamp, V., et al., 2024, Discovery of modern living intertidal stromatolites on Sheybarah Island, Red Sea, Saudi Arabia: Geology, v. XX, p. , https://doi.org/10.1130/G51793.1

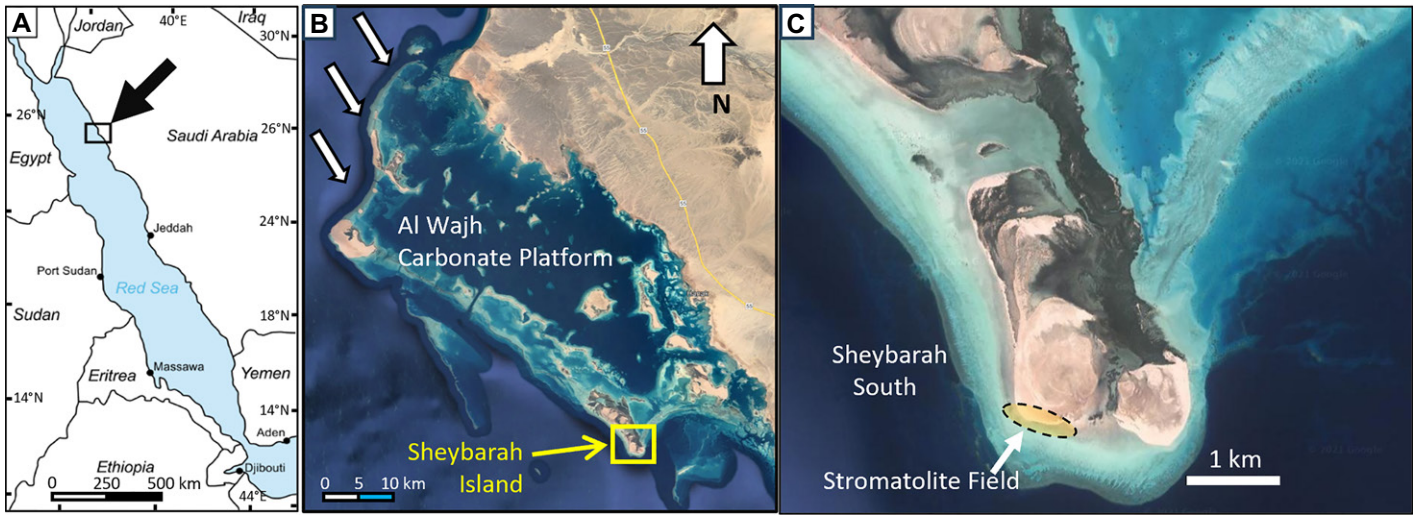

Figure 1. (A) Location of study area in northern Red Sea. (B) Sheybarah Island in SW Al Wajh carbonate platform. White arrows indicate prevailing wind direction based on annual average wind data over 10 yr. (C) Location of stromatolite field at southwestern extent of Sheybarah Island.

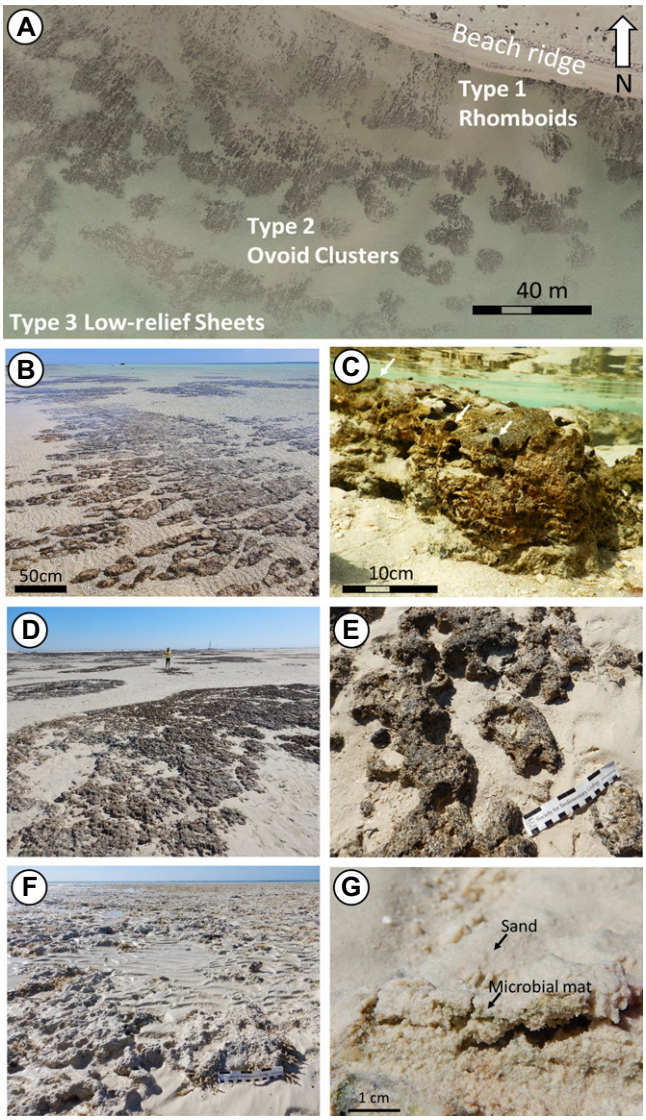

Figure 2. (A) Drone survey image of stromatolite fields, showing three main morphotypes of stromatolites and their distributions. (B–C) Type 1 stromatolites in upper intertidal zone, with elongated sinusoidal to rhomboidal morphology, laminated internal structures, and pustular exterior. White arrows show grazing gastropods during high tide (underwater photo). (D–E) Type 2 stromatolites, consisting of low-relief, irregularly shaped ovoid clusters of stromatolites in the outer field. (F–G) Type 3 stromatolites, composed of less-defined, low-relief microbial mats covered by a thin coating of carbonate sand.

acquisition methodologies are presented in Items S1–S3 in the Supplemental Material[1]. Field data acquisition methods included in situ temperature and salinity logging, a manual field survey, and drone surveys (see Item S1A). Laboratory analysis included X-ray micro–computed tomography (μCT), optical microscopy of thin sections, scanning electron microscopy (SEM), powder X-ray diffraction (XRD), and ^{14}C dating. Preliminary investigation of bacterial community composition was also performed using 16S rRNA gene metabarcoding followed by Illumina sequencing.

ENVIRONMENTAL SETTING

The Sheybarah stromatolite field is in the intertidal to shallow subtidal zone on a gently seaward-dipping fossil reef flat. The age of the underlying coral pavement is mid-Holocene based on ^{14}C age dating of a coral from a shallow core drilled into the reef flat (5264 yr B.P.). This age period relates to the +2 m Holocene sea-level highstand 8000–4000 yr ago reported by Khanna et al. (2021). Eroded domal coral heads suggest that wave energy has lowered the former reef flat to the current sea level. Lithified sands underneath the stromatolites have been dated with ^{14}C as 1640 yr B.P., while the laminations in the stromatolites date between 325 and 120 yr B.P. (see Supplemental Material for all age data). This indicates an onset of stromatolite growth some 300–400 yr ago, or more recently if grains eroded from the mid-Holocene reef flat have been included into the stromatolite fabric.

[1]Supplemental Material. Detailed methodology description for field and laboratory data acquisition. Please visit https://doi.org/10.1130/GEOL.S.25180655 to access the supplemental material; contact editing@geosociety.org with any questions.

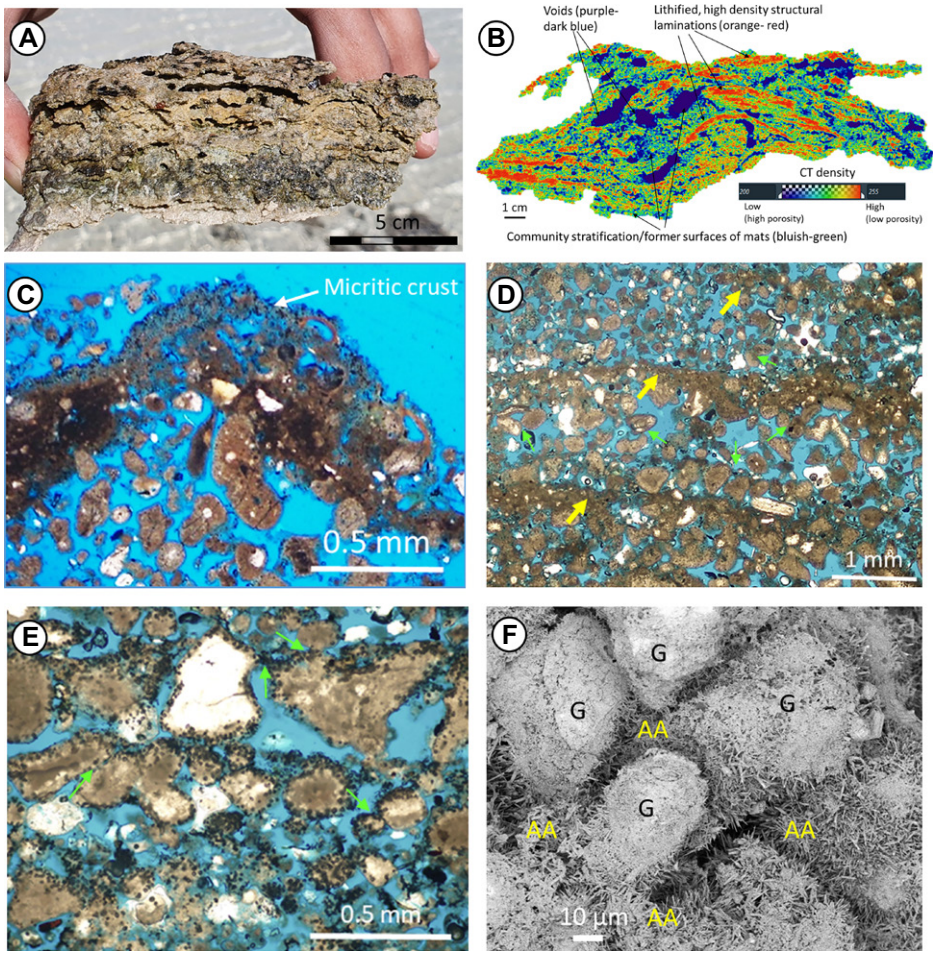

Figure 3. (A) Hand sample of type 1 stromatolite demonstrating layered structures. (B) X-ray micro–computed tomography (µCT) X-Z cross-section image of type 1 stromatolite exposing denser internal laminations (red). Color bar represents range of µCT values corresponding to CT density; blue = void. (C) Thin-section micrograph illustrating micritic crust at surface of stromatolite. (D) Millimeter-scale lithified sediment grain layers (yellow arrows) and fused grains (green arrows). (E) Grains infested with microborings near outer rims and fused at grain contacts (green arrows). (F) Acicular needle aragonite cements (AA) formed around the grain (G) rims.

The daily tidal range is 50–60 cm, reaching a maximum of 1 m. Rare flood surges can inundate lower-lying parts of the island. Sea-surface water temperatures over a year's cycle measured nearby at a water depth of 5 m vary between 21 °C and 31 °C. However, in the intertidal zone, seasonal and daily temperature ranges are more extreme, varying from 8 °C to >48 °C, and reflecting the daily changes caused by seawater inundation and exposure and winter-night/summer-day air temperatures. The average values of salinity, pH, and dissolved oxygen measured during high tide (March 2021) were 42 ppt, 7.8 ± 0.1, and 5.9 ± 0.5 mg/L, respectively. The environmental conditions of the Red Sea are still considered normal, even though salinity is elevated due to the water-circulation patterns and the lack of precipitation.

AREAL EXTENT AND MORPHOTYPES

The Sheybarah stromatolites are distributed over an area exceeding 5 ha (Figs. 1C and 2A). We distinguished stromatolites in the upper intertidal zone adjacent to the beach covering ~3000 m^2 and in the mid-intertidal to shallow subtidal zones (Fig. 2A). There are three main growth forms (Fig. 2A): Type 1—Light gray-green to dark brown, elongated-sinusoidal to rhomboidal structures aligned perpendicular to wave crests, with a height of <15 cm, length of 10–100 cm, and width of 5–50 cm, are found in the upper intertidal zone, often coalescing to larger elongated clusters up to 10 m in length (Fig. 2B). They are pustular on the outside and moderately well lithified (Fig. 2C). Type 2—The mid- to lower intertidal zones are composed of low-relief (height <5 cm), irregularly shaped, ovoid to tabular clusters up to 100 m^2 in area, and these are often anchored by a slightly elevated core of an eroded late Holocene coral (Figs. 2D–2E). Type 3—Poorly lithified, low-relief, irregularly shaped stromatolites occur in the lower intertidal to shallow subtidal zones, commonly covered by a thin coat of white carbonate sand (Figs. 2F–2G).

INNER FABRICS

Herein, we describe the inner structures of type 1 stromatolites (Fig. 3; Fig. S1.2). Cross-section cuts of hand samples and µCT analysis of type 1 stromatolites revealed moderately well-laminated, undulating sediment layers interrupted by vugs and clotted fabrics, suggesting that they are thrombolitic stromatolites sensu Riding (2011) (Figs. 3A and 3B; Item S2.1). Dense lithified layers stand out in relief in cut and washed cross sections and are characterized by high CT density values. Grazing and encrusting borers such as gastropods were often encased during the accretion and lithification of the stromatolite layers (Fig. S2.2). Millimeter-scale laminations are clearly visible in thin-section micrographs and are composed of micritic crusts sandwiched by 1–2-mm-thick sediment accretion layers (Figs. 3C–3D). The sediment grains were micritized to the extent of complete obliteration of the original grain fabric. Layers of fused grains with indistinguishable grain boundaries are common, often underlying micritic crusts (Figs. 3D–3E). The fused grain layers are often infested by microborings, particularly near the rims of the grains, suggesting ongoing micritization even after sediment accretion (Fig. 3E). Elongated acicular aragonite needle rim cements typically <10 µm long are abundant, either occurring as single rods or in meshes perpendicular to grain surfaces (Fig. 3F). The mineral components of the stromatolite layers are aragonite (85%), high-magnesian calcite (9%), and low-magnesian calcite (5%), with minor quantities of quartz and clay minerals (Fig. S2.3).

MICROBIAL DIVERSITY

Filamentous cyanobacteria represent the most abundant bacterial structures as observed through the SEM technique (Figs. 4A–4D). They envelop the sediment grains as single strings or bunches covered by mucous sheaths and biological matrixes consistent with extracellular polymeric substance (EPS) (Figs. 4A–4D; Westall et al., 2000; Dohnalkova et al., 2011). Sub-micron-size equant Ca-Mg–carbonate crystals are abundantly present on the cyanobacterial filaments and EPS (Fig. 4B). Besides filamentous cyanobacteria, other microbial features can be observed, including copious amounts of biofilm-like structures comprising bacterial cells and matrixes compatible with EPS (Fig. 4C), *Navicula*-like diatoms (Fig. 4D), and *Chroococcus*-like structures. Among the most remarkable microbial features are reticulated filaments (Melim et al., 2015), which are ubiquitous in the upper and lower surfaces of the topmost microbial mat layers (Fig. 4E). At the phylum level, the bacterial communities inhabiting the stromatolite structures are dominated by Proteobacteria (49%), with Alphaproteobacteria (30%), Gammaproteobacteria (12%), and Deltaproteobacteria (7%)

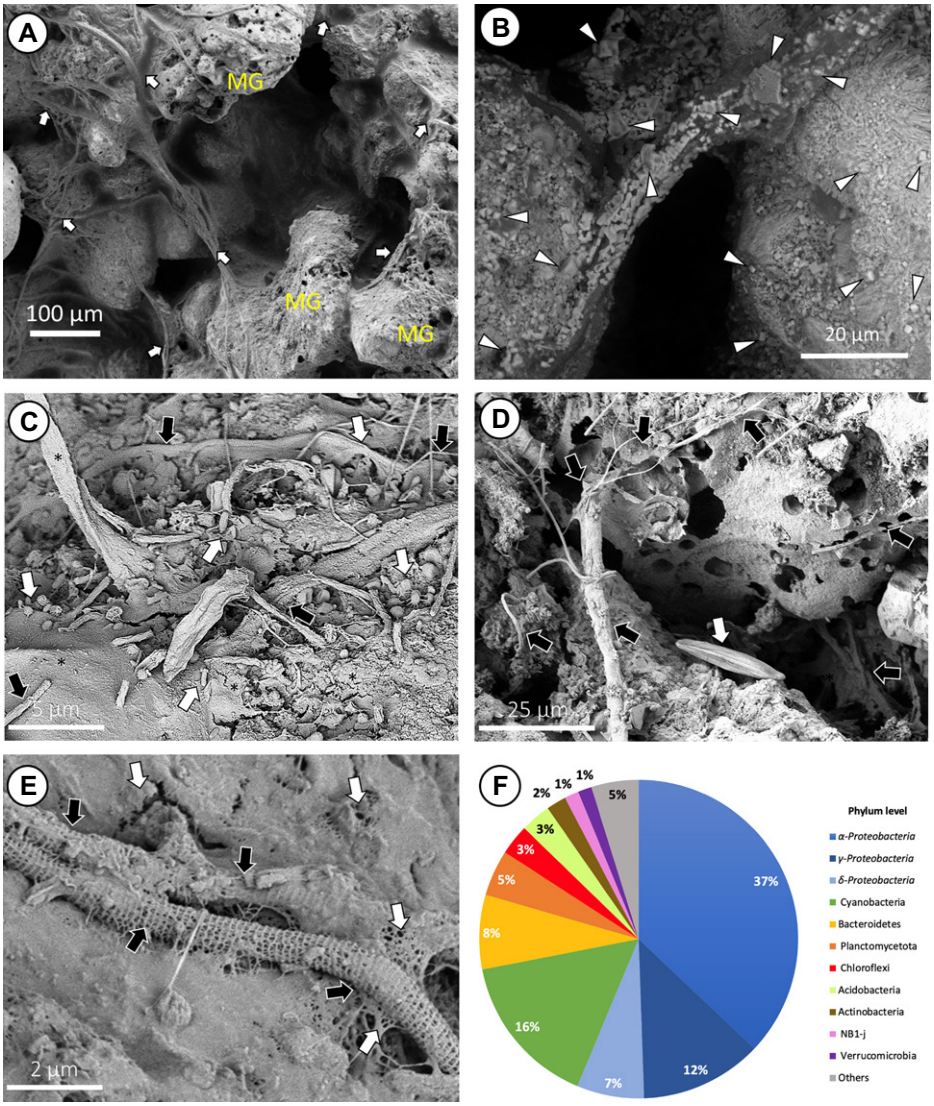

Figure 4. (A–E) Representative scanning electron micrographs showing (A) extensively microbored sediment grains (MG) wrapped in cyanobacterial filaments and extracellular polymeric substance (EPS) films (arrows); (B) High magnesium calcite microcrystals (triangles) associated with cyanobacterial filaments; (C) filamentous structures, possibly bunches and strings of cyanobacteria (black arrows), and single cells of various shapes (white arrows) surrounded by desiccated EPS; (D) filamentous structures of different dimensions (black arrows), surrounding bored surface of sand grain. A diatom is also present (white arrow); and (E) reticulated filaments (black arrows) surrounded by copious amounts of EPS (white arrows). (F) Microbial diversity of Sheybarah Island stromatolites.

as dominant classes, Cyanobacteria (16%), and Bacteroidetes (11%) (Fig. 4F).

DISCUSSION AND CONCLUSIONS

The occurrence of a living stromatolite field under open-marine conditions on Sheybarah Island, NE Red Sea, is likely driven by environmental factors. The dominantly intertidal position of the stromatolites exposes them not only to regular wetting and drying conditions, but also to an extreme temperature range between 8 °C and >48 °C. Currents in the shallow intertidal environment of SW Sheybarah Island are light and remain limited to high tides or occasional storm events. Considering that similar environmental conditions prevail in other islands of the Al Wajh carbonate platform, we predict that other stromatolite fields may occur in the region. The overall intertidal to shallow subtidal setting and the oligotrophic conditions are analogous to the microtidal setting in the Bahamas. However, the height of the Sheybarah stromatolites is limited up to 15 cm, potentially due to lower accommodation space attributed to the microtidal conditions. Their lateral extent appears to be limited by competition with red algae and corals, which dominate the backreef subtidal environment.

The growth of Sheybarah stromatolites is primarily attributed to microbially mediated accretion and differential lithification of sediment grains. The diverse range of sediment-microbial microtextural features observed in the Sheybarah stromatolites indicates cycles of grain entrapment by filamentous microbial structures and fused grains, and cementation similar to the intertidal stromatolites in the Bahamas (Reid and Browne, 1991; Browne, 2011; Dupraz et al., 2013; Frantz et al., 2015). Consistently, relative abundances of bacterial operational taxonomic units composing the microbial communities of Sheybarah stromatolites include a combination of photoautotrophic (Cyanobacteria, 16%) and heterotrophic (e.g., taxa capable of sulfate reduction, including Gammaproteobacteria [12%], Desulfobacteriota [0.8%], and Campylobacteriota [0.02%]; Madigan et al., 2014; Florentino et al., 2016) taxa, which can promote different metabolic processes, contributing to the stromatolite formation.

An intriguing aspect of the Sheybarah stromatolites is the presence of reticulated filaments (Fig. 4E), which have so far only been reported from aphotic environments in caves (Melim et al., 2015). In the Sheybarah stromatolites, these enigmatic features are ubiquitously present in the surface microbial mat and are characterized by variable morphologies, including horizontal ridges supported by vertical columnar structures (Fig. 4E). Their biogeochemical nature and their role in the formation and morphological structure of these stromatolites are unclear and will be subjects of ongoing research.

To the best of our knowledge, the discovery of the Sheybarah stromatolites is the first of its kind in the Middle East, presenting an unprecedented opportunity to study their geobiology in this unique geographic region. Modern open shallow-marine stromatolites are sparsely present on the planet, leading to a lack of suitable analogues for their ancient counterparts. The only previously known modern analogue to the open shallow-marine settings, where most Proterozoic stromatolites developed, has so far been recorded in the Bahamian Archipelago (Dill et al., 1986; Reid and Browne, 1991; Reid et al., 1995, 2000). The discovery of the Sheybarah stromatolite field holds important implications, not only in the scientific perspective, but also in terms of ecosystem services and environmental heritage awareness in line with the ongoing projects for sustainability and ecotourism development promoted by Saudi Arabia. The site is currently under consideration for being a dedicated conservation zone.

ACKNOWLEDGMENTS

We acknowledge funding from King Abdullah University of Science and Technology (KAUST) baseline supports to V. Vahrenkamp and D. Daffonchio. We thank Red Sea Global for their support in accessing the field locations. We thank L. Melim and H. Westphal for fruitful discussions regarding reticulated filaments. We thank the reviewers for their constructive comments and feedback to improve the manuscript.

REFERENCES CITED

Bontognali, T.R., Vasconcelos, C., Warthmann, R.J., Bernasconi, S.M., Dupraz, C., Strohmenger, C.J., and McKenzie, J.A., 2010, Dolomite formation within microbial mats in the coastal sabkha of Abu Dhabi (United Arab Emirates): Sedimentology, v. 57, p. 824–844, https://doi.org/10.1111/j.1365-3091.2009.01121.x.

Browne, K.M., 2011, Modern marine stromatolitic structures: The sediment dilemma, *in* Tewari, V.C., and Seckbach, J., eds., Stromatolites: Interaction of Microbes with Sediments: New York, Springer, p. 291–312, https://doi.org/10.1007/978-94-007-0397-1_13.

Carvalho, C., Oliveira, M.I.N., Macario, K., Guimarães, R.B., Keim, C.N., Sabadini-Santos, E., and Crapez, M.A., 2018, Stromatolite growth in Lagoa Vermelha, southeastern coast of Brazil: Evidence of environmental changes: Radiocarbon, v. 60, p. 383–393, https://doi.org/10.1017/RDC.2017.126.

Chalastani, V.I., Manetos, P., Al-Suwailem, A.M., Hale, J.A., Vijayan, A.P., Pagano, J., Williamson, I., Henshaw, S.D., Albaseet, R., Butt, F., and Brainard, R.E., 2020, Reconciling tourism development and conservation outcomes through marine spatial planning for a Saudi Giga-Project in the Red Sea (The Red Sea Project, Vision 2030): Frontiers in Marine Science, v. 7, https://doi.org/10.3389/fmars.2020.00168.

Dasari, H.P., Langodan, S., Viswanadhapalli, Y., Vadlamudi, B.R., Papadopoulos, V.P., and Hoteit, I., 2018, ENSO influence on the interannual variability of the Red Sea convergence zone and associated rainfall: International Journal of Climatology, v. 38, p. 761–775, https://doi.org/10.1002/joc.5208.

Dill, R.F., Shinn, E.A., Jones, A.T., Kelly, K., and Steinen, R.P., 1986, Giant subtidal stromatolites forming in normal salinity waters: Nature, v. 324, p. 55–58, https://doi.org/10.1038/324055a0.

Dohnalkova, A.C., Marshall, M.J., Arey, B.W., Williams, K.H., Buck, E.C., and Fredrickson, J.K., 2011, Imaging hydrated microbial extracellular polymers: Comparative analysis by electron microscopy: Applied and Environmental Microbiology, v. 77, p. 1254–1262, https://doi.org/10.1128/AEM.02001-10.

Dupraz, C., Fowler, A., Tobias, C., and Visscher, P.T., 2013, Stromatolitic knobs in Storr's Lake (San Salvador, Bahamas): A model system for formation and alteration of laminae: Geobiology, v. 11, p. 527–548, https://doi.org/10.1111/gbi.12063.

Florentino, A.P., Weijma, J., Stams, A.J., and Sánchez-Andrea, I., 2016, Ecophysiology and application of acidophilic sulfur-reducing microorganisms, *in* Rampelotto, P.H., ed., Biotechnology of Extremophiles: Advances and Challenges: Cham, Switzerland, Springer, p. 141–175, https://doi.org/10.1007/978-3-319-13521-2_5.

Frantz, C.M., Petryshyn, V.A., and Corsetti, F.A., 2015, Grain trapping by filamentous cyanobacterial and algal mats: Implications for stromatolite microfabrics through time: Geobiology, v. 13, p. 409–423, https://doi.org/10.1111/gbi.12145.

Grotzinger, J.P., and Knoll, A.H., 1999, Stromatolites in Precambrian carbonates: Evolutionary mileposts or environmental dipsticks?: Annual Review of Earth and Planetary Sciences, v. 27, p. 313–358, https://doi.org/10.1146/annurev.earth.27.1.313.

Hickman-Lewis, K., Cavalazzi, B., Giannoukos, K., D'Amico, L., Vrbaski, S., Saccomano, G., Dreossi, D., Tromba, G., Foucher, F., Brownscombe, W., and Smith, C.L., 2023, Advanced two- and three-dimensional insights into Earth's oldest stromatolites (ca. 3.5 Ga): Prospects for the search for life on Mars: Geology, v. 51, p. 33–38, https://doi.org/10.1130/G50390.1.

Jiang, H., Farrar, J.T., Beardsley, R.C., Chen, R., and Chen, C., 2009, Zonal surface wind jets across the Red Sea due to mountain gap forcing along both sides of the Red Sea: Geophysical Research Letters, v. 36, L19605, https://doi.org/10.1029/2009GL040008.

Khanna, P., Petrovic, A., Ramdani, A.I., Homewood, P., Mettraux, M., and Vahrenkamp, V., 2021, Mid-Holocene to present circum-Arabian sea level database: Investigating future coastal ocean inundation risk along the Arabian plate shorelines: Quaternary Science Reviews, v. 261, https://doi.org/10.1016/j.quascirev.2021.106959.

Madigan, M.T., Martinko, J.M., Bender, K.S., Buckley, D.H., and Stahl, D.A., 2014, Brock Biology of Microorganisms (14th ed.): Boston, Pearson, 1064 p.

Maillard, C., and Soliman, G., 1986, Hydrography of the Red Sea and exchanges with the Indian Ocean in summer: Oceanologica Acta, v. 9, p. 249–269.

Marin-Carbonne, J., Decraene, M.N., Havas, R., Remusat, L., Pasquier, V., Alléon, J., Zeyen, N., Bouton, A., Bernard, S., Escrig, S., and Olivier, N., 2022, Early precipitated micropyrite in microbialites: A time capsule of microbial sulfur cycling: Geochemical Perspectives Letters, v. 21, p. 7–12, https://doi.org/10.7185/geochemlet.2209.

Melim, L.A., Northup, D.E., Spilde, M.N., and Boston, P.J., 2015, Update: Living reticulated filaments from Herbstlabyrinth-Adventhöhle cave system, Germany: Journal of Caves and Karst Studies, v. 77, p. 87–90, https://doi.org/10.4311/2015MB0112.

Perri, E., Tucker, M.E., Słowakiewicz, M., Whitaker, F., Bowen, L., and Perrotta, I.D., 2018, Carbonate and silicate biomineralization in a hypersaline microbial mat (Mesaieed sabkha, Qatar): Roles of bacteria, extracellular polymeric substances and viruses: Sedimentology, v. 65, p. 1213–1245, https://doi.org/10.1111/sed.12419.

Petrovic, A., Ariza Fuentes, M., Putri, I., Yahaya, L.N., Khanna, P., Purkis, S.J., and Vahrenkamp, V., 2022, Holocene sediment distribution in the Al Wajh platform lagoon (northern Red Sea, Saudi Arabia), a modern analogue for large rift basin carbonate platforms: Sedimentology, v. 69, p. 1365–1398, https://doi.org/10.1111/sed.12955.

Petrovic, A., Lüdmann, T., Afifi, A.M., Saitz, Y., Betzler, C., and Vahrenkamp, V., 2023a, Fragmentation, rafting, and drowning of a carbonate platform margin in a rift-basin setting: Geology, v. 51, p. 242–246, https://doi.org/10.1130/G50546.1.

Petrovic, A., Reijmer, J.J., Alsaihati, S.H.M., Nommensen, D., and Vahrenkamp, V., 2023b, Sediment dynamics and geomorphology of a submarine carbonate platform canyon system situated in an arid climate setting: Sedimentology, v. 70, p. 2241–2271, https://doi.org/10.1111/sed.13120.

Raitsos, D.E., Pradhan, Y., Brewin, R.J., Stenchikov, G., and Hoteit, I., 2013, Remote sensing the phytoplankton seasonal succession of the Red Sea: PLoS One, v. 8, https://doi.org/10.1371/journal.pone.0064909.

Reid, R.P., and Browne, K.M., 1991, Intertidal stromatolites in a fringing Holocene reef complex, Bahamas: Geology, v. 19, p. 15–18, https://doi.org/10.1130/0091-7613(1991)019<0015:ISIAFH>2.3.CO;2.

Reid, R.P., Macintyre, I.G., Steneck, R.S., Browne, K.M., and Miller, T.E., 1995, Stromatolites in the Exuma Cays, Bahamas: Uncommonly common: Facies, v. 33, p. 1–18, https://doi.org/10.1007/BF02537442.

Reid, R.P., Visscher, P.T., Decho, A.W., Stolz, J.F., Bebout, B.M., Dupraz, C., Macintyre, I.G., Paerl, H.W., Pinckney, J.L., Prufert-Bebout, L., and Steppe, T.F., 2000, The role of microbes in accretion, lamination and early lithification of modern marine stromatolites: Nature, v. 406, p. 989–992, https://doi.org/10.1038/35023158.

Riding, R., 2011, Microbialites, stromatolites, and thrombolites, *in* Reitner, J., and Thiel, V., eds., Encyclopedia of Geobiology. Encyclopedia of Earth Science Series: Springer, Heidelberg, p. 635–654.

Samylina, O.S., and Zaytseva, L.V., 2019, Characterization of modern dolomite stromatolites from hypersaline Petukhovskoe Soda Lake, Russia: Lethaia, v. 52, p. 1–13, https://doi.org/10.1111/let.12286.

Strohmenger, C.J., and Jameson, J., 2018, Gypsum stromatolites from Sawda Nathil: Relicts from a southern coastline of Qatar: Carbonates Evaporites, v 33, p. 169–186, https://doi.org/10.1007/s13146-017-0365-2.

Suosaari, E.P., Reid, R.P., Playford, P.E., Foster, J.S., Stolz, J.F., Casaburi, G., Hagan, P.D., Chirayath, V., Macintyre, I.G., Planavsky, N.J., and Eberli, G.P., 2016, New multi-scale perspectives on the stromatolites of Shark Bay, Western Australia: Scientific Reports, v. 6, https://doi.org/10.1038/srep20557.

Suosaari, E.P., Reid, R.P., Oehlert, A.M., Playford, P.E., Steffensen, C.K., Andres, M.S., Suosaari, G.V., Milano, G.R., and Eberli, G.P., 2019, Stromatolite provinces of Hamelin Pool: Physiographic controls on stromatolites and associated lithofacies: Journal of Sedimentary Research, v. 89, p. 207–226, https://doi.org/10.2110/jsr.2019.8.

Visscher, P.T., Reid, R.P., Bebout, B.M., Hoeft, S.E., Macintyre, I.G., and Thompson, J.A., 1998, Formation of lithified micritic laminae in modern marine stromatolites (Bahamas): The role of sulfur cycling: The American Mineralogist, v. 83, p. 1482–1493, https://doi.org/10.2138/am-1998-11-1236.

Westall, F., Steele, A., Toporski, J., Walsh, M., Allen, C., Guidry, S., McKay, D., Gibson, E., and Chafetz, H., 2000, Polymeric substances and biofilms as biomarkers in terrestrial materials: Implications for extraterrestrial samples: Journal of Geophysical Research–Planets, v. 105, p. 24,511–24,527, https://doi.org/10.1029/2000JE001250.

Printed in the USA